Peer-reviewed version available at J. Mar. Sci. Eng. 2020, 8, 556; doi:10.3390/jmse8080556

Article

Overtopping metrics and coastal safety: a case of study from the Catalan coast

Corrado Altomare [1,2,*], Xavier Gironella [1], Tomohiro Suzuki [3,4], Giacomo Viccione [5], Alessandra Saponieri [6]

[1] Laboratori d'Enginyeria Maritima, Universitat Politècnica de Catalunya – BarcelonaTech, Calle Jordi Girona 1-3, 08034, Barcelona, Spain; corrado.altomare@upc.edu, xavi.gironella@upc.edu
[2] Ghent University, Department of Civil Engineering, Technologiepark 60, 9052 Gent, Belgium
[3] Flanders Hydraulics Research, Berchemlei 115, 2140 Antwerp, Belgium; tomohiro.suzuki@mow.vlaanderen.be
[4] Dept. of Hydraulic Engineering, Delft University of Technology, Stevinweg 1, 2628, CN Delft, the Netherlands
[5] Environmental and Maritime Hydraulics Laboratory (LIDAM), University of Salerno, Via Giovanni Paolo II, 132, 84084 Fisciano SA, Italy; gviccion@unisa.it
[6] University of Salento, Department of Engineering for Innovation, University of Salento, Ecotekne, 73047, Lecce, Italy; alessandra.saponieri@unisalento.it
* Correspondence: corrado.altomare@upc.edu; Tel.: +34-93-401-70-17

Abstract: Design criteria for coastal defenses exposed to wave overtopping are usually assessed by mean overtopping discharges and maximum individual overtopping volumes. However, it is often difficult to give clear and precise limits of tolerable overtopping for all kind of layouts. A few studies analyzed the relationship between wave overtopping flows and hazard levels for people on sea dikes, confirming that one single value of admissible mean discharge or individual overtopping volume is not a sufficient indicator of the hazard, but detailed characterization of flow velocities and depths is required. This work presents the results of an experimental campaign aiming at characterizing the flow characteristics associated to maximum individual overtopping volumes for an urbanized stretch of a town along the Catalan coast, where a walking and bike path and a railway run along the coastline are exposed to significant overtopping events every stormy season. The work compares different safety criteria for pedestrian. Results prove that safety of pedestrian on a sea dike can be still guaranteed even for overtopping volumes larger than 1000 l/m. Pedestrian hazard is rather proved to be linked to the combination of overtopping flow velocity and flow depth.

Keywords: wave overtopping; coastal safety; flow velocity; flow depth; sea dikes

1. Introduction

Wave overtopping assessment is a key procedure within the general design of any coastal defense. The groundwork for the assessment of wave overtopping was laid by [1], who chose the average discharge as design value, stating that "there is no such thing as an absolute discharge: because the wave heights and periods exhibit a random distribution about a given mean, the discharge will also vary randomly". Since [1], several experimental campaigns have been carried out worldwide, leading to semi-empirical models, which are nowadays largely used for wave overtopping assessment (e.g. [2]–[4]). Nevertheless, during the last few years the increased storminess caused by climate change has raised concerns among researchers, engineers and decision-makers: is the average overtopping an appropriate design criterion? Or are the biggest waves to cause the major damages and casualties? Allsop et al. [5] highlighted that tests on the effects of overtopping flows on people indicate that the assessment of mean discharge is not enough to evaluate people safety; the authors proposed maximum individual overtopping volumes as more suitable hazards

Peer-reviewed version available at J. Mar. Sci. Eng. 2020, 8, 556; doi:10.3390/jmse8080556

indicators. Limits for individual overtopping volumes together with tolerable mean discharges were proposed in [5] related to overtopping velocities below 10 m/s. Yet the authors suggested that lower volumes may be required for violent overtopping processes with higher velocities. Therefore, it was emphasized but not discussed further that other flows parameters might play an important role and be linked to overtopping hazards namely overtopping flow velocity and overtopping flow depth. Generally speaking, "the character of overtopping flow hazards depends on geometries of the defence, the hinterland and the form of overtopping" [5]. Several studies have been gathered and presented in EurOtop [6], where finally a tolerable limit for maximum individual volumes equal to 600 l/m is suggested, over which a single event cannot be tolerate by people (Table 1).

Table 1. Tolerable overtopping limits for people proposed in EurOtop (2018).

Hazard type and reason	**Mean discharge, q (l/s/m)**	**Maximum individual volume V_{max} (l/m)**
People at structures with possible violent overtopping, mostly vertical structures	No access for any predicted overtopping	No access for any predicted overtopping
People at seawall / dike crest. Clear view of the sea.		
H_{m0}=3m	0.3	600
H_{m0}=2m	1	600
H_{m0}=1m	10-20	600
H_{m0}<0.5m	No limit	No limit

Despite many efforts have been done to assess overtopping flow velocities and overtopping flow depths on the seaward side, crest and landward side of coastal defenses [6]–[10], no direct link has been clearly established between tolerable overtopping individual volumes and discharges with tolerable flow velocities and flow depths.

Few studies considered overtopping flow depths and velocities in order to estimate the overtopping hazard for pedestrians [11], [12]. In some case, the referred limits were obtained from physical experiments using anthropomorphic dummies, in other cases [12] a video analysis of real flooding events has been performed. Besides, any formula for overtopping flow depth and velocity does not refer necessary to the same specific overtopping event, since the 2% exceedance probability of the two quantities is considered. These quantities are proved to be not correlated [10]. Nevertheless, when looking at the maximum individual overtopping volumes, the aim is to characterize the flow depth and velocity associated to that volume, since it is the one reported as threshold value for safety [6].

The present work analyses the overtopping discharges, volumes, overtopping flow depth and velocities that can lead to risk scenarios for people. The work is focusing on coastal defenses in highly urbanized areas. For the purpose, the case study of Premià de Mar is analyzed, which schematically represents the coastline north of Barcelona, Spain. In Premià de Mar, a railway, bike and pedestrian path are located very close to the coastline and are exposed every winter season to considerable events. The main purpose of this study is to discuss the validity of the present safety limits and design criteria for the Catalan coast. To reach this objective, physical model tests were carried out, modelling a layout that resembles the case study for different wave conditions corresponding to events with different return periods. The acquired experimental data were collected, analyzed and compared with the state-of-the-art semi-empirical formulas; the results, finally, were compared with the safety criteria from [6] and with the stability curves for people combining flow velocities and depths [12]–[14].

2. Overtopping flow parameters and people safety

The scientific literature available on wave overtopping prediction is very extensive. There are, however, few reports dealing with the stability of people under the effect of wave overtopping flows, that is limited to a modest number of studies. In this area of investigation, some studies have tested human subjects in controlled flow conditions which have generated a quantification of the critical flows parameters and mechanisms, possibly leading a person losing stability and fall in the surrounding flow. The first study with the purpose to analyze the human stability in wave overtopping flows, was promoted by the Japanese Port and Harbor Research Institute (PHRI), the results of which are published in [11]. The authors proposed two models of human instability: "slipping" and "tumbling". The first one occurs when the flow force against the body (F_f) is bigger than the maximum available bottom friction resistance of the subject (F_r). The second mechanism models the falling process rising when the unbalancing moment produced by the flow around the feet of the subject is bigger than the restoring moment produced by the weight of the person (M_r). Sandoval and Bruce [12] revisited the model of [11], accounting for the buoyancy of the subject, as well as its related position respect to the incoming flows. The analysis for each mechanism of instability can be derived as follows:

1. Friction stability (F_f-F_r)

$$u^2 \cdot d = \frac{2 \cdot \mu \cdot m_g \cdot g}{C_d \cdot \rho \cdot B1} \quad (1)$$

2. Momentum stability (M_r-M_f)

$$u \cdot d = 2\sqrt{\frac{d_1 \cdot m_g \cdot g}{C_d \cdot \rho \cdot B1}} \quad (2)$$

with:
u=flow velocity (m/s);
d=flow depth (m);
ρ=density of water (kg/m^3);
μ=coefficient of friction between shoe sole and ground (-);
B_1=average diameter of the subject legs (m);
C_d=drag coefficient (-)
d_1=distance from pivot point to the center gravity (m);
m_g= subject's mass (kg)

The moments generated by the flows (M_f) can be calculated as the drag force applied at the half of the depth. On the other hand, the restoring moment (M_r) is a function of the person weight and the distance to the pivot point (d_1).

More recently, Arrighi et al. [13]-[14] compared the experimental evidences for humans and vehicles with the results of a numerical investigation. The authors identified relative submergence and Froude number, as the most relevant parameters to express the vulnerability of pedestrians. They derived a regression curve for human stability expressed as follows:

$$\frac{H_{crP}}{H_P} = \frac{0.29}{0.24+Fr} \quad (3)$$

where H_{crP} is the critical flow depth, H_P is the height of the subject, while their ratio represents the relative submergence. If $H/H_{crP}<1$, the person is stable. The Froude number is calculated as $u/\sqrt{gd}$.

3. Overtopping flow velocity and flow depth estimation on the dike crest

There is already plenty of literature dealing with the estimation of overtopping flow parameters [10], [15], [16]. The equations for overtopping flow depth and velocity at the dike crest can be expressed in a general form as follows:

Preprints (www.preprints.org) | NOT PEER-REVIEWED | Posted: 9 July 2020 doi:10.20944/preprints202007.0164.v1

Peer-reviewed version available at J. Mar. Sci. Eng. 2020, 8, 556; doi:10.3390/jmse8080556

$$d_{2\%} = c_{d2\%}(Ru_{2\%} - R_c)exp\left(-c_{c,d}\frac{x_c}{B}\right) \quad (4)$$

$$u_{2\%} = c_{u2\%}(Ru_{2\%} - R_c)exp\left(-c_{c,u}\frac{x_c\mu}{2d_{2\%}}\right) \quad (5)$$

where $d_{2\%}$ is the overtopping flow depth on the dike crest, $u_{2\%}$ is the overtopping flow velocity on the dike crest, x_c is the streamwise coordinate on the dike crest, μ is the bottom friction coefficient, $Ru_{2\%}$ is the wave run-up, R_c is the crest freeboard respect to the still water level (Figure 1). The subscript 2% refers to quantities exceeded by 2% of the number of the incident waves. The coefficients $c_{d2\%}$, $c_{u2\%}$, $c_{c,d}$, and $c_{c,u}$ are empirical coefficients, the values can vary according to the literature. For run-up assessment, formulas are here omitted for sake of simplicity. Reader can refer, for example, to [6].

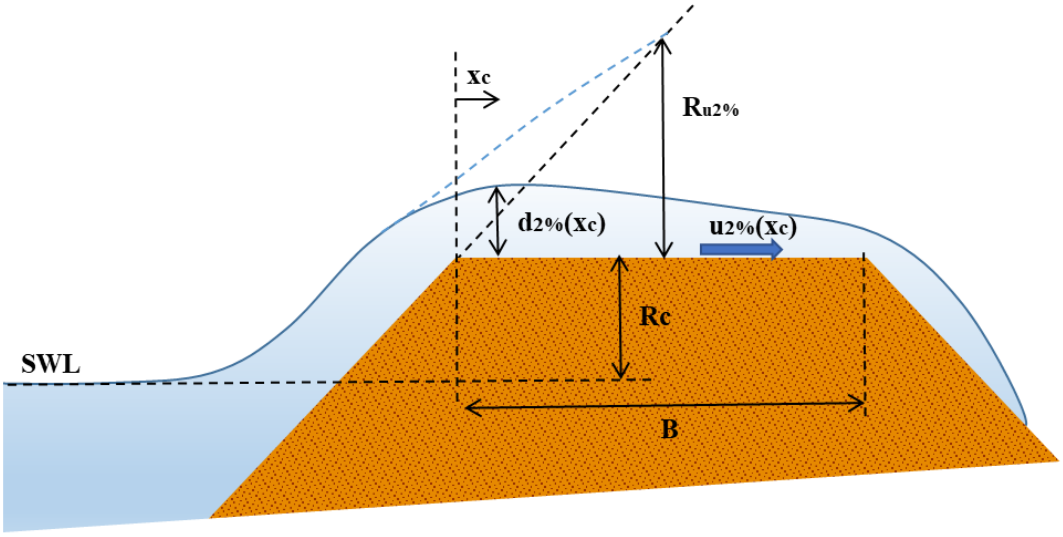

Figure 1. Scheme of overtopping flow on a sea dike.

Instead, Hughes [17] established empirical relationships between individual overtopping wave volumes and the maximum velocity, maximum flow depth and individual discharge, based on data for 1:3 and 1:6 dike slope:

$$u = 27.67\frac{\sqrt{V_{max}tan\alpha}}{T_{m-1,0}} \quad (6)$$

$$d = 0.324\sqrt{V_{max}} \quad (7)$$

$$q_{max} = 7.405V_{max}\frac{\sqrt{tan\alpha}}{T_{m-1,0}} \quad (8)$$

In this case *u* and *d* refer to the maximum velocity and depth on the dike crest, respectively. The dike slope and the wave period are included in the relationship, but most important there is a direct link with the individual overtopping volume. This is also confirmed by [18] who derived expressions for overtopping flow parameters analytically based on wave momentum flux, in analogy with [19].

4. Model

Physical model experiments were carried out in the CIEMito wave flume at the Maritime Engineering Laboratory of Universitat Politècnica de Catalunya – BarcelonaTech (LIM/UPC). The geometrical layout used for the experimental campaign resembles the beach and coastal protection in the area of Premià de Mar, municipality in the Comarca of the Maresme in Catalonia, Spain. This stretch of the coast is characterised by the presence of both railways and a promenade/bike path very exposed to possible sea storms, being located at a few meters from the shoreline. A dike made of natural stone with a relatively steep slope (1:1) characterises this coastal area. In the physical model tests, the effects

Preprints (www.preprints.org) | NOT PEER-REVIEWED | Posted: 9 July 2020 doi:10.20944/preprints202007.0164.v1

Peer-reviewed version available at J. Mar. Sci. Eng. 2020, 8, 556; doi:10.3390/jmse8080556

of the rubble mound have been neglected, considering a smooth slope, instead. It is interest of the present research to analyses those stretches where nourishment was no longer performed (characteristic in winter season and respectively, storm events). Hence, the beach has been eroded, leaving exposed directly the dike to the sea. A bathymetric survey was carried out with a sailing drone built at LIM/UPC. A water depth at the dike toe was between 0.5 and 1m and the crest of the dike is 3-4m above the mean sea level. Based on the measurement, two different foreshore slope were considered for this study, namely 1:15 (steep) and 1:30 (gentle) to represents the coast of Premià de Mar.

4.1. Case of study and model geometry

The wave flume is 18 m long, 0.38 m wide and 0.56 m high. The wave generation system is a piston-type board. The support structure consists of square metal sections and both laterals and bottom walls are made of tempered glass which allows a complete view of the tests and clear video camera recording.

The model (scale is 1:50) was built and operated according to Froude's similarity law. A sketch of the layout is proposed in Figure 2, where all dimensions are in model scale. The model consists of a 1:n transition slope followed by a 1:m foreshore slope, where n is equal to 8 for m=15 and 5 for m=30, respectively. A 1:1 smooth dike made of polymethyl methacrylate is located at the end of the foreshore. Dike height is 0.09 m. Different widths for the promenade (i.e. crest berm) were modelled, namely 0.12 and 0.24 m, to be representative of the different stretches along the coastline. The freeboard varies between 0.061 m and 0.081 m, with toe depths of 0.009-0.029 m (Table 2).

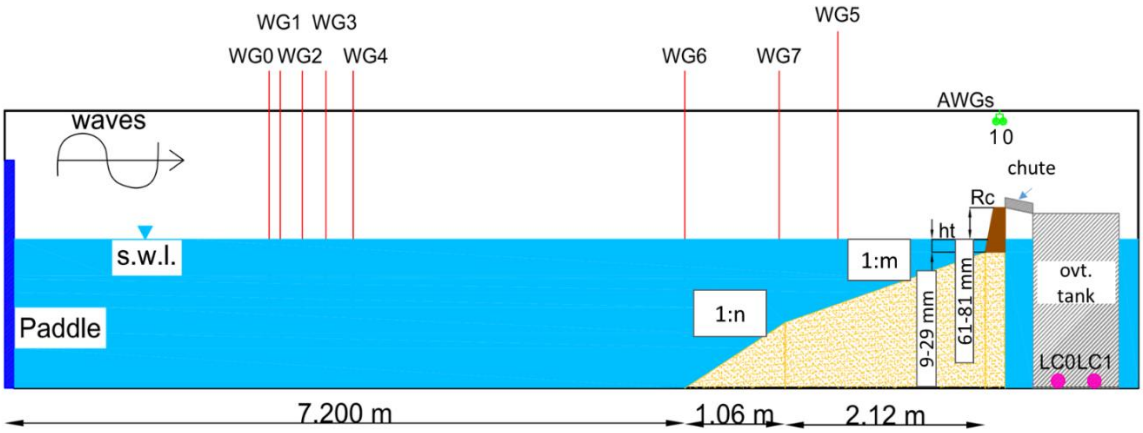

Figure 2. CIEMito wave flume – drawing of the longitudinal section (distorted). Dimensions are in model scale. The value of m is equal to 15 and 30 respectively. Accordingly, n assumes values of 8 and 5 respectively.

Irregular wave tests, employing a JONSWAP spectrum with enhancement factor equal to 3.3, were performed. Each test consisted in approximately 1000 waves. In total 420 tests were conducted. We consider 243 tests for the present analysis, having excluded those ones with no or inaccurate overtopping flow property measurements. The tested wave conditions were derived from the extreme wave forecast based on data acquired by the buoy of the Puertos del Estado, located outside Barcelona harbour, for return periods of 1, 2, 5 and >10 years. These conditions correspond to very shallow and extremely shallow water conditions, based on the definition in [20], being $h_{toe}/H_{m0,o}$ between 0.1 and 0.38, where h_{toe} is the water depth at the dike toe and $H_{m0,o}$ is the offshore wave height.

Table 2. Geometric characteristics of the tested dike layout.

Scale	h_{toe} (m)	R_c (m)	Promenade width (m)
Model	0.009-0.019-0.024-0.029	0.81-0.071-0.066-0.061	0.12-0.24
Prototype	0.45-0.905-1.2-1.45	4.05-3.55-3.3-3.05	6-12

The experimental tests carried out are aimed to measure the following parameters: free surface water elevation along the wave flume, η (m); cumulated overtopping volume, V_{tot} (l/m); mean

Peer-reviewed version available at J. Mar. Sci. Eng. 2020, 8, 556; doi:10.3390/jmse8080556

overtopping discharge, q (l/s/m), obtained as $V_{tot}/T_{mm-1,0,o}*N_{w,o}$, where $T_{mm-1,0,o}$ is the spectral wave period close to the wave generation (offshore) and $N_{w,o}$ is the number of waves offshore; maximum overtopping volume, V_{max} (l/m); flow depth associated to the maximum overtopping volume, d (m); horizontal velocity associated to the maximum overtopping volume, u (m/s).

4.2. Case of study and model geometry

Eight resistive sensors were placed along the flume to measure the water surface elevation at different location (WG0-WG8), working at a sample frequency of 80 Hz. Distance of the resistive wave gauges with respect to the mean paddle position are reported in Table 3.

Table 3. Location from paddle of resistive wave gauges (in meters)

Sensor	**WG0**	**WG1**	**WG2**	**WG3**	**WG4**	**WG6**	**WG7**	**WG5**
x (m=15)	2.8	2.96	3.15	3.40	3.69	7.20	8.20	9.20
x (m=30)	2.8	2.96	3.15	3.40	3.69	7.20	8.20	9.20

Overtopping flow depth and overtopping flow velocity were measured by means of redundant systems, composed of two high-speed cameras and two ultrasonic sensors. Results were compared and averaged. Two ultrasonic sensors were place on the dike top to measure flow depths (AWG0, AWG1), with resolution <0.3 mm. AWG 1 is positioned 2.5 cm far from the dike edge for the crest width of 0.12 m and 6 cm for the crest width of 0.24 cm. Distance between AGW1 and AWG0 varied between 5.9 cm and 9.2 cm. The position of the two ultrasonic sensors and the vertical distance from the crest were optimized case per case to avoid interference between the sensors and optimize accuracy. The AWG raw signal was acquired with a sampling rate of 100 Hz and filtered in Matlab environment in order to derive overtopping flow depth and velocity on the dike. The velocity was calculated with the indirect methodology:

$$u_{AWGt_{tip}} = \frac{distance_{AWG}}{\Delta t_{tip}}, \; u_{AWGt_{max}} = \frac{distance_{AWG}}{\Delta t_{max}} \tag{9}$$

where the delta values are, respectively the temporal distance between the two maximum points Δt_{max} and the distance between the two starting points of the event Δt_{tip}. The latter ones correspond to a threshold value of 1mm, which identifies the tip of the overtopping wave. An example of the time series of flow depth for a maximum overtopping event is depicted in Figure 3, where the solid line is the acquisition of the sensor at the end of the promenade (AWG0) and the dashed line is the registration of the sensor at the beginning of the promenade (AWG1). Maximum of each signal is marked with a circle. Threshold values are marked with diamond markers. Here a clarification is required. The overtopping volumes are measured after the dike promenade. Hence, flow depth and velocity associated to maximum event refers to the same location. For flow depth, the signal of AWG0 is used, being the closest sensor to the end of the promenade. However, as described previously, velocity is measured indirectly and the calculation employs both ultrasonic sensors. The distance between AWG1 and AWG0 is comparable to the promenade width, therefore the calculated velocity cannot be considered as instantaneous velocity at the promenade end. Therefore, the layer velocity associated to the maximum volume and corresponding to the maximum flow depth, d_{AWG0}, has been calculated resolving the following system, considering momentum conservation:

$$\begin{cases} d_{AWG1}u_{AWG1} = d_{AWG0}u_{AWG0} \\ u_{AWGt_{max}} = \frac{u_{AWG1}+u_{AWG0}}{2} \end{cases} \tag{10}$$

where $u_{AWGtmax}$ is the average velocity as previously described, d_{AWG0} and d_{AWG1} are the maximum flow depth values at AWG0 and AWG1 location respectively, u_{AWG0} and u_{AWG1} are the instantaneous velocities associated to d_{AWG0} and d_{AWG1}. For all analysis reported in the next sections, we will refer to d_{AWG0} and d_{AWG1} as maximum flow depth d and overtopping flow velocity u, for sake of simplicity.

Preprints (www.preprints.org) | NOT PEER-REVIEWED | Posted: 9 July 2020 doi:10.20944/preprints202007.0164.v1

Peer-reviewed version available at J. Mar. Sci. Eng. 2020, 8, 556; doi:10.3390/jmse8080556

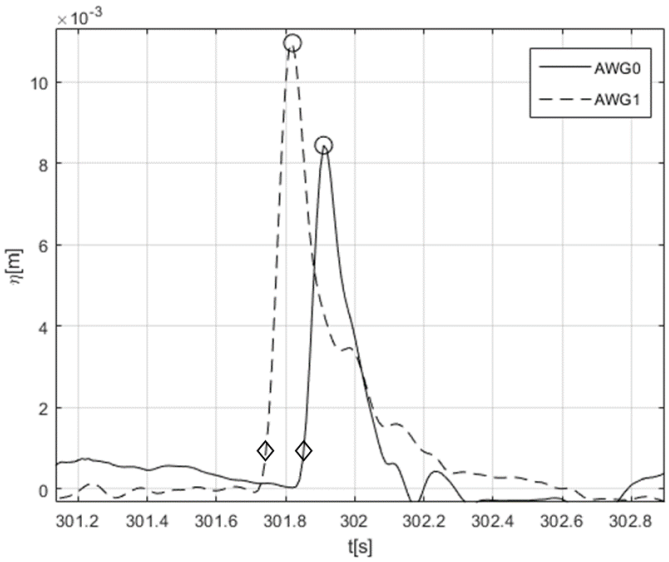

Figure 3. Example of simultaneous time series recorded by ultrasonic sensors.

The high-speed cameras were working at 200 fps. They were placed in order to provide top and lateral view of the overtopping flows on the dike crest. The camera 1 was placed on the top of the structure. The dike promenade was graduated with equally spaced lines (1 cm). The camera 2 was placed in front of the lateral glass wall, on the side of the sea-dike model, where a transparent paper graduated with 0.5 cm squares was placed. From camera 1, only layer velocity could be measured as $s/\Delta t$, where s corresponds to the distance measured on the reference 1cm frame equal to the distance between the two ultrasonic sensors; Δt is the time needed for the tip of the overtopping flow to run such a distance. From camera 2, flow velocity and depth were measured: the lateral view allowed to identify both the tip of the overtopping wave and the height of the overtopping layer (Figure 4). Results were compared with the ultrasonic sensors (Figure 5).

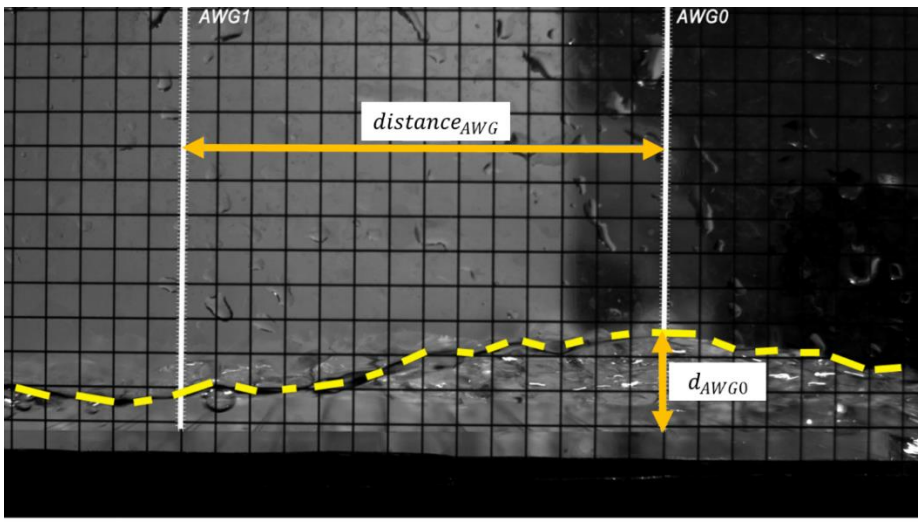

Figure 4. Lateral view with high-speed camera (CAM2).

Same considerations for instantaneous and average velocities are made for the cameras' measurements. Figure 5 plots the correlation between the measurements of maximum flow depth carried out by means of ultrasonic sensors and high-speed camera (CAM2). Data are divided according to the foreshore slope. A correlation coefficient R^2 between 52% and 73% is calculated, showing good agreement between measurements.

Preprints (www.preprints.org) | NOT PEER-REVIEWED | Posted: 9 July 2020 doi:10.20944/preprints202007.0164.v1

Peer-reviewed version available at J. Mar. Sci. Eng. 2020, 8, 556; doi:10.3390/jmse8080556

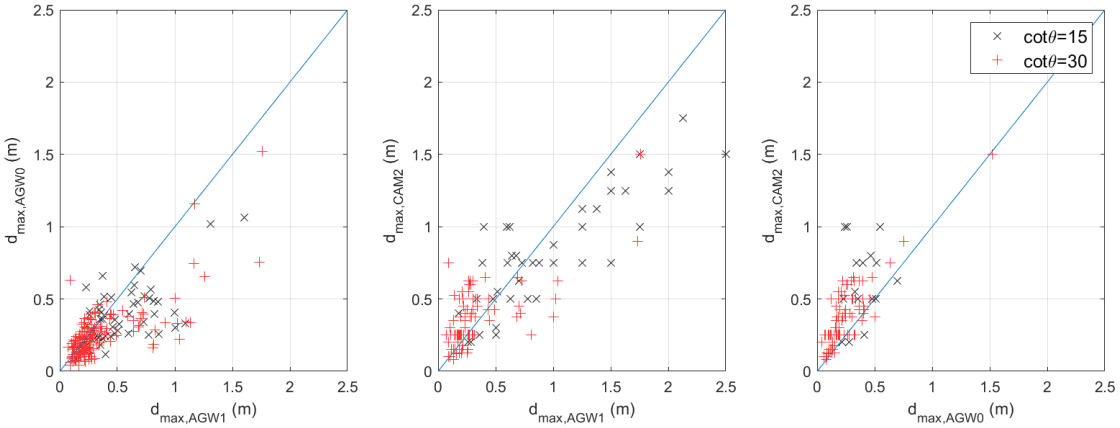

Figure 5. Correlation between overtopping flow depths measured with ultrasonic sensors and high-speed cameras.

The individual and mean overtopping volume was collected inside an isolated metallic water box, connected to the edge of the promenade by a 9 cm wide chute. Two load cells were installed under the overtopping tank located into the box in order to measure the cumulated water weight, with an acquisition frequency of 20 Hz. The volume was obtained by dividing weight by water density.

4.3. Wave analysis

Classical linear reflection analysis methods are not suitable in shallow water conditions because non-linear effects are dominant [4], since generation of low-frequency waves is dominant and affects the value of the mean wave period $T_{m-1,0}$. This wave period is shown to be important for many wave-structure interaction processes, and can be used to assess the response of coastal structures with shallow foreshores [20], [21]. Hence, the dike was removed and horizontal bottom followed by absorption material was placed, instead, to measure incident wave conditions at the dike toe, which are required for the analysis. Sensor WG5 was used for the scope.

A limitation in the experiments is the use of first-order wave generation and the lack of active absorption of long-wave energy. For spurious long waves in the flume, the lack of a second-order wave generation is found to be negligible due to relative large water depth at the wave generator and low steepness [22]. The natural frequency of the current flume set-up is around 0.045-0.05 Hz for different test conditions and foreshore slopes, which are found to be outside of the frequency range of the infragravity waves in the flume. Moreover, there is no increasing trend of the observed long-wave energy at the toe of the dike. A passive absorption system was found to be sufficient to reduce the wave reflection, except for the seiching motion. The frequency at the seiching frequency band was removed in the analysis of the wave parameters.

4.4. Scale effects

The employed model scale is relatively small and can rise concerns on possible scale effects that might affect wave overtopping. Heller [24] provides an overview of limiting criteria flow-structures interaction phenomena and shows typical applied scales for the investigation, which are good compromise between reasonable model size and moderate scale effects. However, based on this classification scale effects are not necessarily negligible and need further investigation. Therefore, the influence of viscous forces and surface tension has been analysed, accordingly to what reported in [6] and [8]. The Reynolds and Weber numbers for wave overtopping (R_{eq} and W_{eq}) have been calculated. Results have been compared versus the proposed critical limits, namely $R_{eq} > 10^3$ and $W_{eq} > 10$. In total 25 cases show a $R_{eq}<10^3$ and $W_{eq}<10$. Further analysis was carried out to quantify scale effects on those cases following two different methodologies: 1) a correction for the model scale, based on [8] was calculated; 2) Artificial Neural Network (ANN) proposed by [24] has been employed and predicted

Preprints (www.preprints.org) | NOT PEER-REVIEWED | Posted: 9 July 2020 doi:10.20944/preprints202007.0164.v1

Peer-reviewed version available at J. Mar. Sci. Eng. 2020, 8, 556; doi:10.3390/jmse8080556

overtopping discharges have been compared with the measured ones. Both methodologies prove that scale effects can be neglected. The correction calculated with [8] method ranged between 1 and 1.1. ANN predictions show values in the same order or just smaller than experimental ones. Further details are here omitted for sake of simplicity.

5. Results

5.1. Relationship between mean discharge, individual volumes and overtopping flow parameters

Figure 6 shows the relationship between mean overtopping discharge and maximum individual overtopping volume. Data are divided according to the slope of the foreshore. For the same mean discharge, the maximum individual volume is smaller for the 1:30 foreshore slope than for 1:15 foreshore slope: heavy breaking caused by gentle foreshore and shallow water conditions provoke more energy dissipation and reduce the chance of very big individual overtopping events. The steeper slope is characterized by less but more intense overtopping events, meanwhile the gentle slope experiences more events but smaller in magnitude. This suggests that overtopping processes on milder slopes are somewhat less violent, in agreement with analysis proposed in Chapter 3 of EurOtop [6]. The thresholds proposed by EurOtop for people safety (Table 1) are drawn in Figure 6, both in terms of mean discharge and maximum volume. It is important to notice that meanwhile tolerable discharge values vary depending on the local wave conditions at the dike toe, for maximum volume the threshold is fixed at 600 l/m with no further considerations. Almost all experimental results show volumes higher than the proposed limit, however all values of mean discharge are within the limits of 10-20 l/s/m, value suggested for wave height at the dike toe equal to 1m (same order of results got during the experimental campaign). This inconsistency will be discussed later.

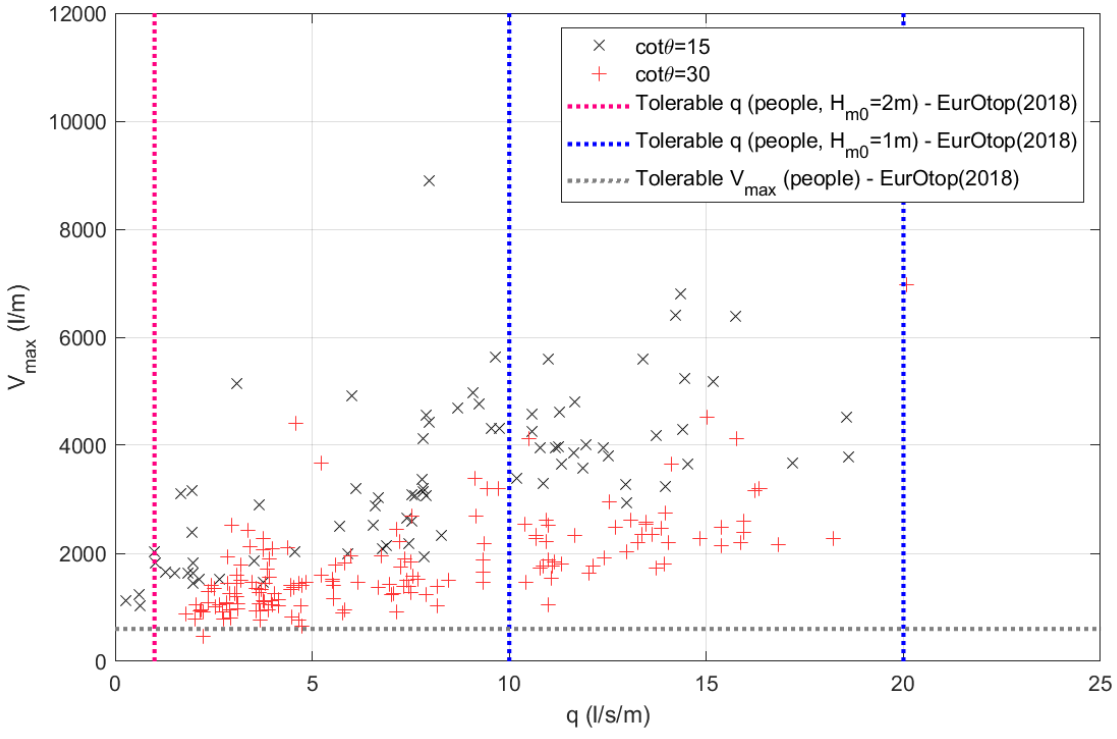

Figure 6. Variation of maximum individual overtopping volume with mean discharge (dimensions in prototype). Limits for safety of pedestrians and assets based on EurOtop (2018) are shown. The two vertical blue lines correspond to tolerable discharges of 10 and 20 l/s/m respectively, for Hm0=1m.

The relationship between q and V_{max} seems pretty linear, whereas more dispersion can be noticed looking the overtopping flow depth and velocity behavior versus individual overtopping volume

Preprints (www.preprints.org) | NOT PEER-REVIEWED | Posted: 9 July 2020 doi:10.20944/preprints202007.0164.v1

Peer-reviewed version available at J. Mar. Sci. Eng. 2020, 8, 556; doi:10.3390/jmse8080556

(Figure 7). This is especially true for the 1:15 foreshore slope, where more intense overtopping events are far more energetic and violent than the ones for 1:30 slopes.

It must be remarked that the measured overtopping flow velocities are not necessarily the highest velocities recorded during overtopping process, but they are the ones associated to the overtopping event characterized by the maximum individual volume. In agreement with [17] and [18], a correlation between overtopping flow parameters and individual maximum volumes is noticeable, differently from mean overtopping discharges (Figure 8) where larger scatters are noticed.

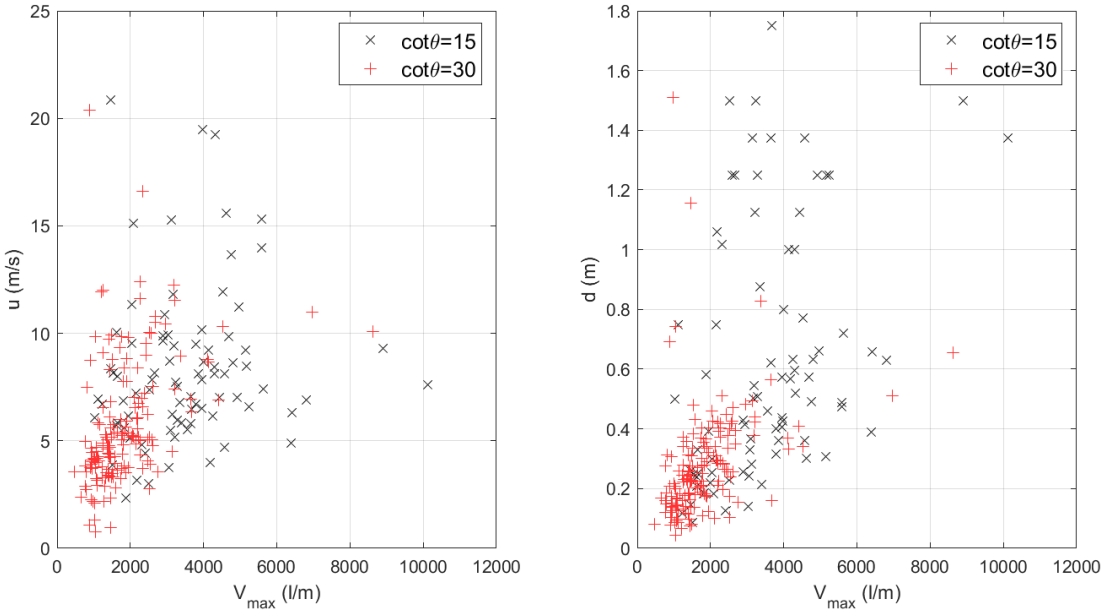

Figure 7. Variation of overtopping flow velocity and depth with maximum individual overtopping volume (dimensions in prototype) for two different foreshore slopes.

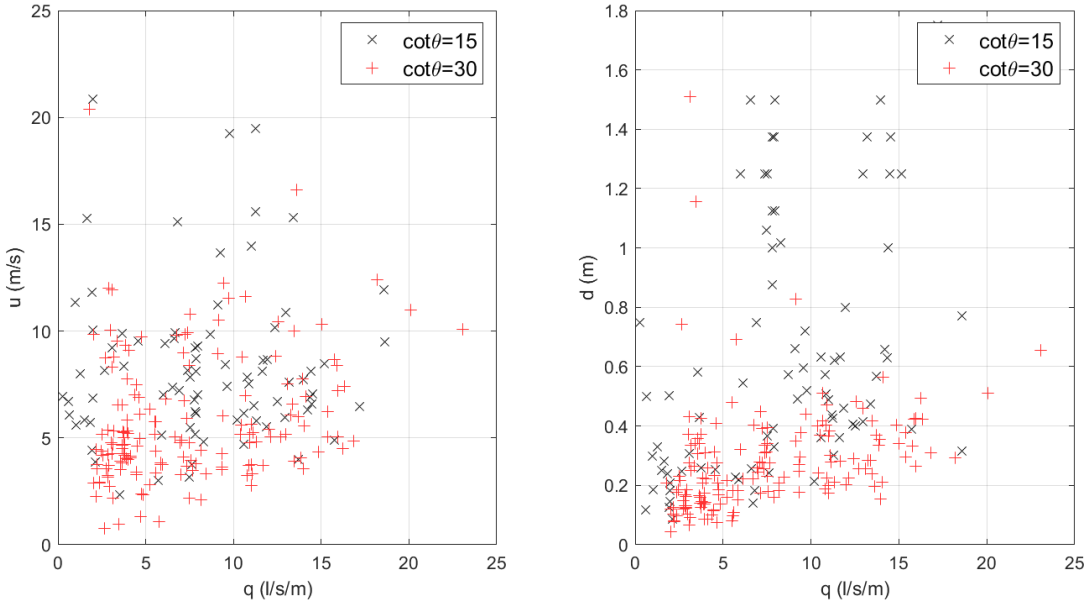

Figure 8. Variation of overtopping layer velocity and depth with average overtopping discharge (dimensions in prototype) for two different foreshore slopes.

Preprints (www.preprints.org) | NOT PEER-REVIEWED | Posted: 9 July 2020 doi:10.20944/preprints202007.0164.v1

Peer-reviewed version available at J. Mar. Sci. Eng. 2020, 8, 556; doi:10.3390/jmse8080556

To better understand the possible correlation among variables a dimensional analysis has been carried out. Stand to the Buckingham's π theorem, if there are n variables in a problem containing k primary dimensions, the equation relating all the variables will have n-m dimensionless groups. In mathematical terms, it is possible to write:

$$f(H_{m0}, T_{m-1,0}, h_{toe}, u, d, q, V_{max}, R_c, g, tan\theta_{eq}, B) = 0 \quad (10)$$

where H_{m0} and $T_{m-1,0}$ are the spectral wave height and period at the dike toe respectively, h_{toe} is the water depth at the dike toe, B is the width of the dike promenade, g is the gravity acceleration, q is the average overtopping discharge, V_{max} the maximum individual overtopping volume expressed in l per meter of crest width, R_c the crest freeboard, u and d the overtopping flow velocity and depth. The parameter $tan\theta_{eq}$ corresponds to the equivalent slope, calculated starting from the dike and foreshore slope for cases with foreshores in shallow water conditions as indicated in [25]. Hence, n=11 and k=2, leading to 9 dimensionless parameters:

$$f\left(\frac{H_{m0}}{h_{toe}}, \frac{T_{m-1,0}}{\sqrt{gh_{toe}}}, \frac{B}{d}, \frac{tan\theta_{eq}}{\sqrt{\frac{H_{m0}}{\frac{g}{2\pi}T^2_{m1-,0}}}}, \frac{u}{\sqrt{gh_{toe}}}, \frac{d}{H_{m0}}, \frac{q}{\sqrt{gH^3_{mo}}}, \frac{V_{max}}{\frac{g}{2\pi}H_{m0}T^2_{m1-,0}}, \frac{R_c}{H_{m0}}\right) = 0 \quad (11)$$

The selection of each dimensionless group is based on current literature and intends to be physically meaningful. As for example, the wave period and the overtopping flow velocity have been divided by the square root of gh_{toe} corresponding this quantity to the wave celerity in shallow waters. Identification of dimensionless groups will help to investigate possible relationships between overtopping flow depth and velocity with other variables at stake. The relationship between overtopping flow depth and velocity with individual maximum overtopping volumes, has been investigated in terms of dimensionless groups as shown in Figure 9. It is possible to distinguish two different trends, one per foreshore slope. Lower values of the dimensionless velocity are shown for a wide range of volumes in case of the 1:30 slope. Opposite to that, a wide variation of velocity is shown within a relative short range of volumes for the steeper foreshore. A more careful analysis of the results shows actually that the overtopping flow depth is greatly affected by the promenade width (see Figure 10), which does not show a clear correlation with overtopping flow velocity.

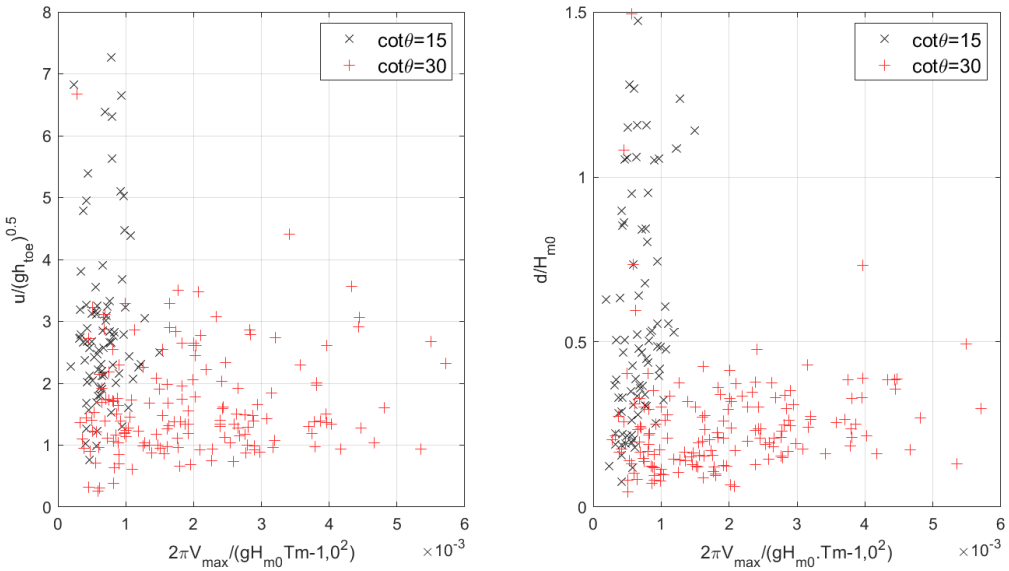

Figure 9. Variation of dimensionless overtopping layer velocity and depth with dimensionless maximum individual overtopping volume for two different foreshore slopes.

Preprints (www.preprints.org) | NOT PEER-REVIEWED | Posted: 9 July 2020 doi:10.20944/preprints202007.0164.v1

Peer-reviewed version available at J. Mar. Sci. Eng. 2020, 8, 556; doi:10.3390/jmse8080556

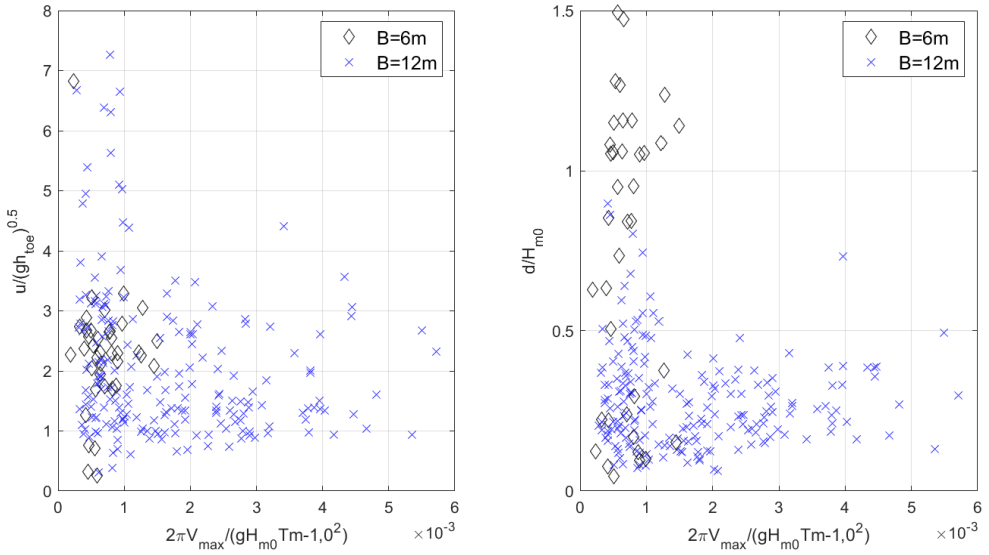

Figure 10. Variation of dimensionless overtopping layer velocity and depth with dimensionless maximum individual overtopping volume for two different promenade width.

Results for overtopping flow depth and velocity have been compared with formulas proposed in [26], [6] and [18], who finally express both overtopping flow parameters as function of wave run-up and crest freeboard. The application of the aforementioned methods requires an estimation of the run-up. Notwithstanding, wave run-up assessment for very and extremely shallow waters and relative steep dikes cannot avoid inaccuracies, due to the fact that experimental data fall outside the rang of application of any known semi-empirical formula to calculate $R_{2\%}$ or R_{max}. Results are depicted in Figure 11 where it is clear that poor agreement is found between experimental results and calculated values.

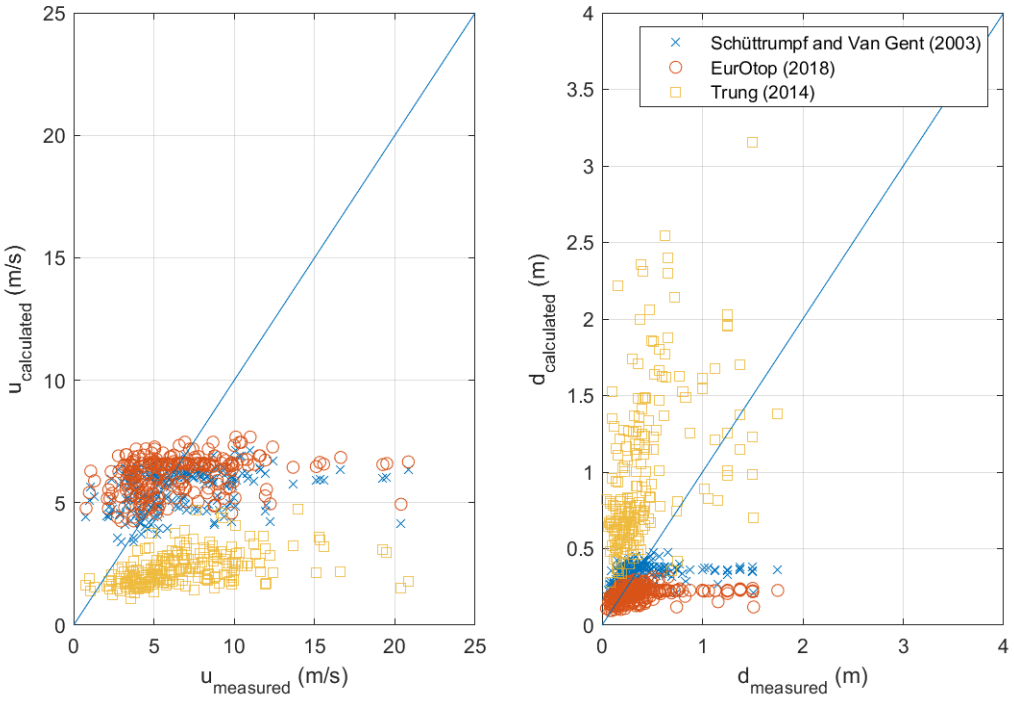

Figure 11. Estimation of overtopping flow depth and velocity employing existing formulas from Schüttrumpf and Van Gent (2003), Trung (2014) and EurOtop (2018).

Preprints (www.preprints.org) | NOT PEER-REVIEWED | Posted: 9 July 2020 doi:10.20944/preprints202007.0164.v1

Peer-reviewed version available at J. Mar. Sci. Eng. 2020, 8, 556; doi:10.3390/jmse8080556

5.2. Overtopping flow parameters expressed in terms of individual maximum overtopping volume

The application of the formulas proposed by Hughes [17], being function of the maximum individual overtopping volume are considered more adequate to be applied to the presented results, without further sources of uncertainty. It must be noticed that [17] analyzed overtopping flow parameters only at the seaward edge of the dike crest and not along it. The effects of the crest width are therefore neglected. Comparisons are reported in Figure 12: unlike overtopping flow depth, flow velocities and discharges are considerably under predicted. Possible explanation is the influence of the spectral wave period: $T_{m-1,0}$ can be found at the denominator of Eqs 6-8, however the measured wave periods are far larger than the one tested in [17], as deeply affected by heavy breaking and release and shift of the spectral energy to very low frequency as result of the release of infra-gravity waves for very and extremely shallow water conditions.

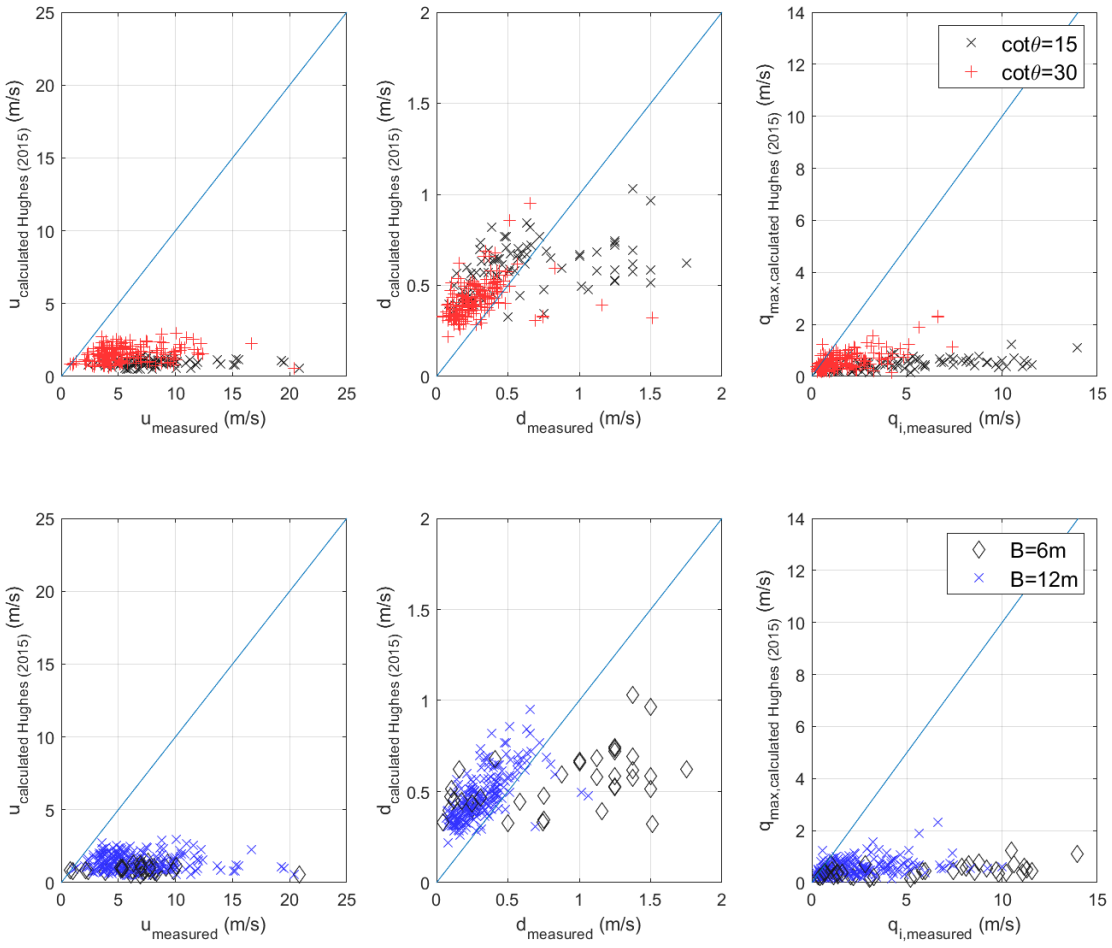

Figure 12. Estimation of overtopping flow depth and velocity employing formulas from Hughes (2015).

Mares-Nasarre et al. [10] demonstrated that overtopping flow velocity and flow depth are correlated if we look at them in statistic terms; they appear to be independent when related to the same individual overtopping event. Notwithstanding, we aimed to further investigate possible correlations among dimensionless valuable. For the scope, the Evolutionary Polynomial Regression (EPR) technique by [27] has been employed. EPR implements a multi-modelling approach with multi-objective genetic algorithm. This technique was already successfully applied to coastal engineering problems [28], [29] to find a simple and easily interpretable mathematical models that express the reflection coefficient variation for irregular waves for a particular low-reflective caisson breakwater. After several iterations, the following expressions have been found for overtopping flow depth, overtopping flow velocity and individual overtopping discharge:

Preprints (www.preprints.org) | NOT PEER-REVIEWED | Posted: 9 July 2020 doi:10.20944/preprints202007.0164.v1

Peer-reviewed version available at J. Mar. Sci. Eng. 2020, 8, 556; doi:10.3390/jmse8080556

$$u_{calculated\ EPR} = 0.254\sqrt{V_{max}\frac{gR_c}{H_{m0}}} \quad (12)$$

$$d_{calculated\ EPR} = 0.343\sqrt{V_{max}\frac{H_{m0}\xi_{m-1,0}}{R_c x_c}} \quad (13)$$

$$q_{max,calculated\ EPR} = 0.25V_{max}\sqrt{\frac{g\xi_{m-1,0}}{x_c}} \quad (14)$$

Similar dependence on the individual overtopping volume is found by employing EPR as by [18] and [17]. Besides, a certain influence of the location where flow parameters are measured xc, surf similarity parameter $\xi_{m-1,0}$ and dimensionless freeboard R_c/H_{m0} results from the analysis. The surf similarity parameter is here calculated employing the equivalent slope as defined in [25]. The influence of the freeboard might be explained as follows: for the same volume, higher freeboard will lead to lower flow depths (run-up is lower). Besides, the surf similarity parameter will be bigger for longer periods (i.e. bigger wavelengths), leading to bigger individual discharges.

Measured overtopping flow parameters are plotted against the calculated ones in Figure 13. Big scatter is noticed especially for those cases with steeper foreshore slope and narrower crest width: the more violent overtopping events, often characterized by splashes and jets, makes more difficult to measure overtopping flow properties without errors (R^2 is about 50%). In any case, it is important to emphasize here that it is not intended to find new relationships for the overtopping flow parameters to overcome or upgrade the ones already proposed in literature. The EPR analysis is carried out to provide rather a general overview of the possible correlations among variables and help to interpret the results. Larger databases are required to optimize any regression for the flow properties on the dike crest but this is out of scope of the present work.

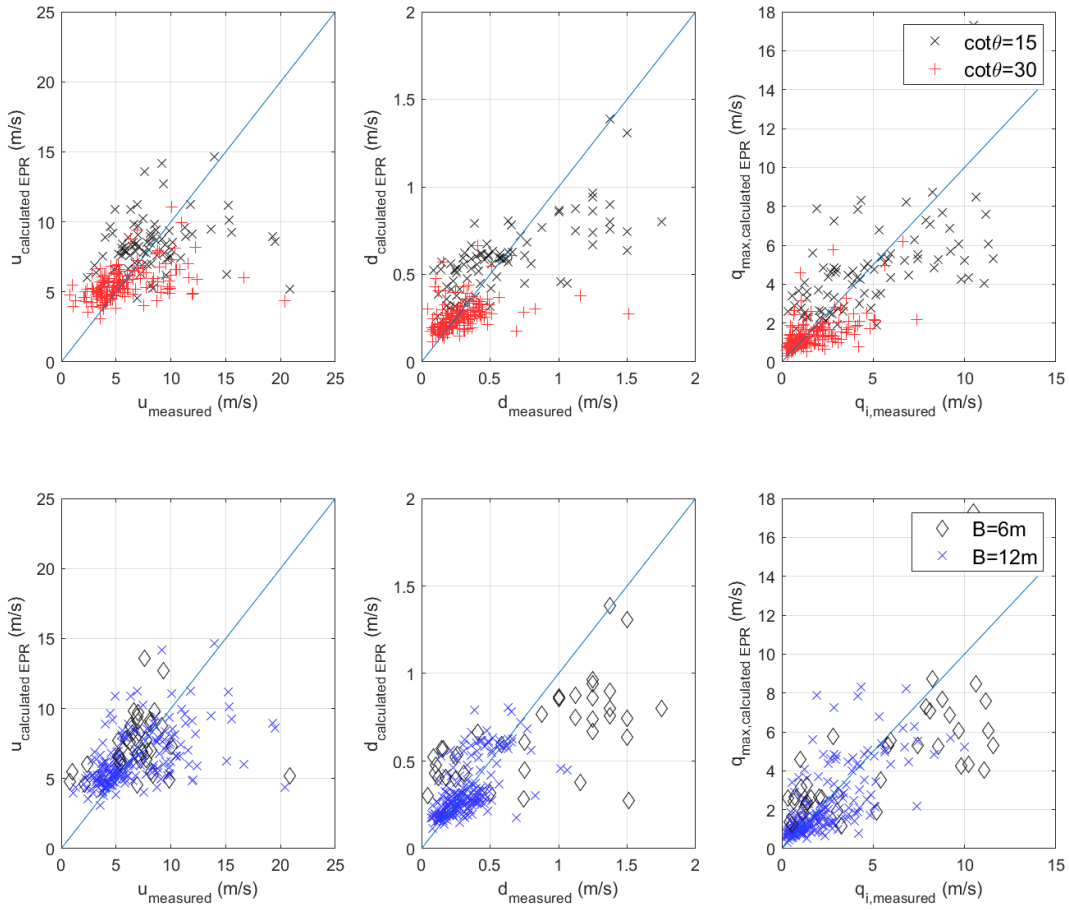

Figure 13. EPR results for overtopping flow properties on the dike crest versus measured ones.

6. Analysis and comparison of safety criteria and limits of wave overtopping for design of sea dikes

In the previous section, possible correlation among the aforementioned variables has been shown. Overtopping flow velocity and flow depth show a clear dependence on the individual volume, as also confirmed by [17], [18]. Poor correlation is noticed with the mean overtopping discharge, instead. Usually, the only overtopping variables considered during the design of any coastal defense are the mean discharge and the maximum volume. According to [6], people standing and walking on or behind a coastal defense can be considered safe when the volume and discharges values are within certain limits: a preliminary comparison of the obtained experimental data with the tolerable limits of Table 1 has been shown in Figure 6. Results indicate that: 1) the measured values of volumes are bigger than the proposed threshold, except for a very few cases; 2) mean overtopping discharge is always within the proposed thresholds.

Considering the limit on individual volume stronger condition than the one on discharge, it can be concluded that [6] limits are not verified for this particular case. However, a deeper look at overtopping flow properties leads to different conclusions. The safety conditions are evaluated through the stability curves proposed by Sandoval and Bruce [12] and Arrighi et al. [14]. Results are plotted in Figure 14 and Figure 15, respectively. Data are categorized in terms of crest width and mean overtopping discharges, based on [6] ($q<5$; $5<q<15$; $q>15$ l/s/m). Moreover, Figure 16 and Figure 17 show the same comparison but data are gathered in three different groups depending on the maximum individual overtopping volume ($V_{max}<1000$; $1000< V_{max} <5000$; $V_{max} >5000$ l/m). Stability curves calculated for a male adult person and 10 years old child are plotted in Figure 14 and Figure 16. All data above the safety curves lie in an unsafe region, whereas all data below the lines correspond to safe flow conditions.

Looking at overtopping flow properties, it becomes clear that overtopping safety criteria based on mean discharge and maximum volume are not sufficient and might lead to over predict the hazards related to overtopping events. Although almost all cases present individual maximum volumes higher than 600 l/m, at least 20% of them can be considered safe if looking at combination of flow velocity and depth. The influence of the berm width is remarkable: for shorter berm almost, all cases with V_{max}>1000 l/m fall within the unsafe region (above the curves in the figures), while the same volume can be not so critical for longer berms, for which actually the results are more scattered. Cases with V_{max} >1000 l/m that lead to unsafe flows are those with mean discharge q>5/l/s/m, a part from a few exceptions. In general, very high discharges and volumes, respectively greater than 10 l/s/m and 5000 l/m, lead to unsafe flows for both considered promenade widths.

The results show that the design of costal defenses must fulfil certain conditions that aim to guarantee the safety of people on or behind coastal defenses. These conditions cannot be reduced to the overtopping assessment of mean discharges and maximum volumes. Assessment of overtopping flow velocity and flow depth is required, in order to upgrade the current design criteria. To evaluate the flow velocity and depth associated to the maximum overtopping event is not an easy task and any semi-empirical model that can be derived would be limited to specific hydrodynamic conditions and geometrical layouts. Instead, experimental or, as alternative, numerical modelling provide a further insight into the processes occurring on the dike crest.

Preprints (www.preprints.org) | NOT PEER-REVIEWED | Posted: 9 July 2020 doi:10.20944/preprints202007.0164.v1

Peer-reviewed version available at J. Mar. Sci. Eng. 2020, 8, 556; doi:10.3390/jmse8080556

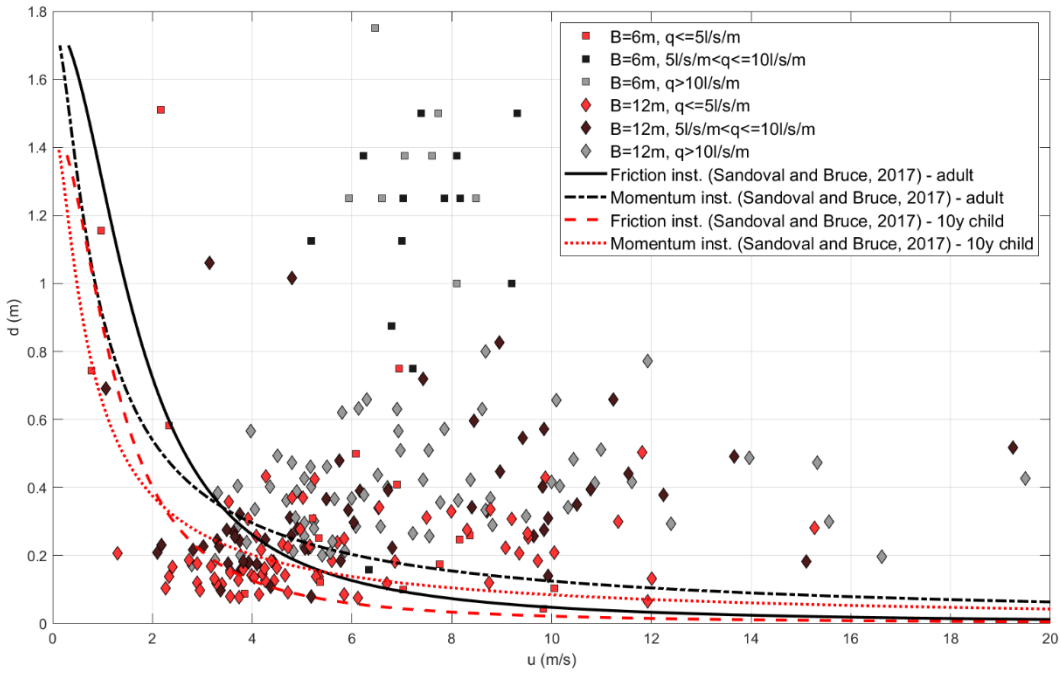

Figure 14. Flow depth versus velocity, comparison with Sandoval and Bruce (2017) curves, the discharges are divided for different promenades and measured average discharge.

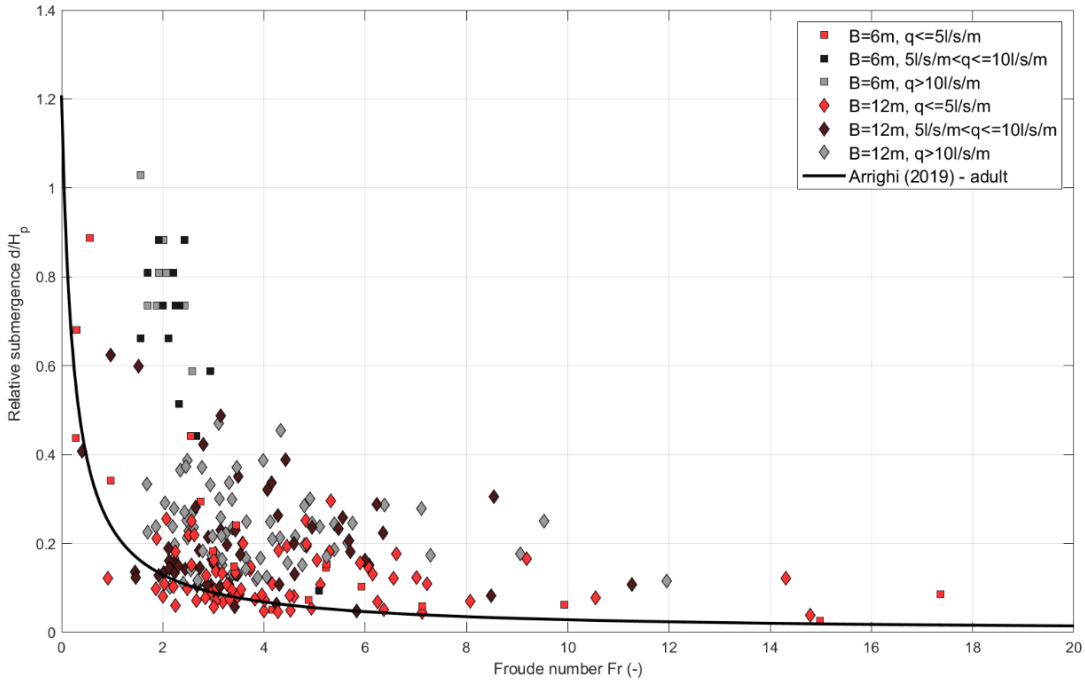

Figure 15. Froude number versus relative submergence, comparison with Arrighi (2017) curve, the discharges are divided for different promenades and measured average discharge.

Preprints (www.preprints.org) | NOT PEER-REVIEWED | Posted: 9 July 2020 doi:10.20944/preprints202007.0164.v1

Peer-reviewed version available at J. Mar. Sci. Eng. 2020, 8, 556; doi:10.3390/jmse8080556

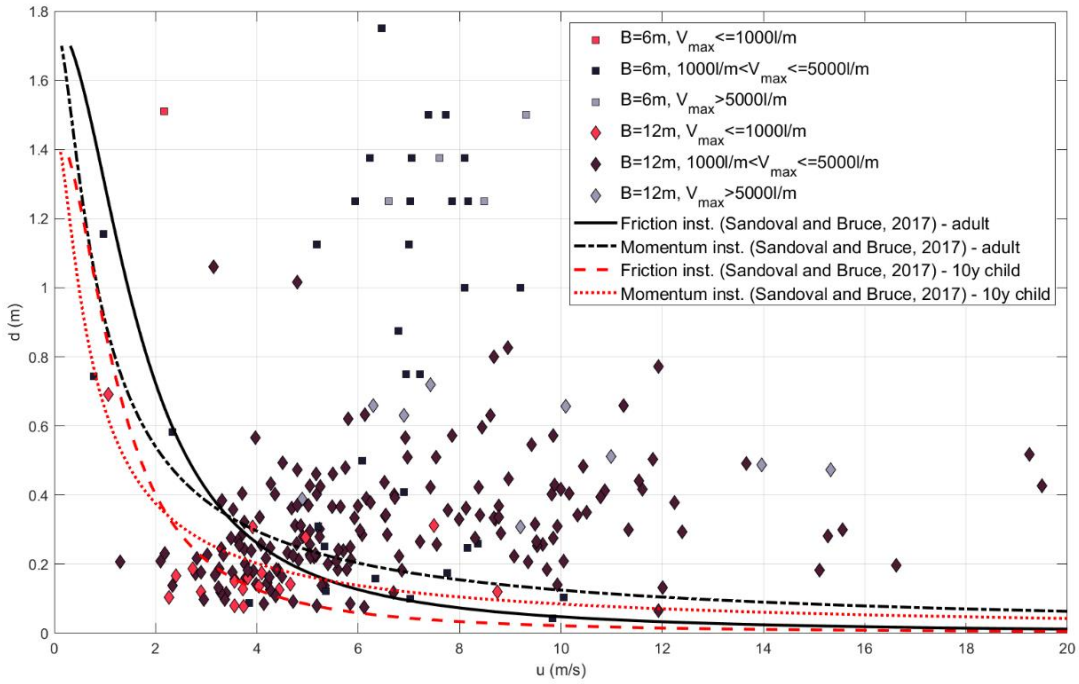

Figure 16. Flow depth versus velocity, comparison with Sandoval and Bruce (2017) curves, the discharges are divided for different promenades and maximum volumes.

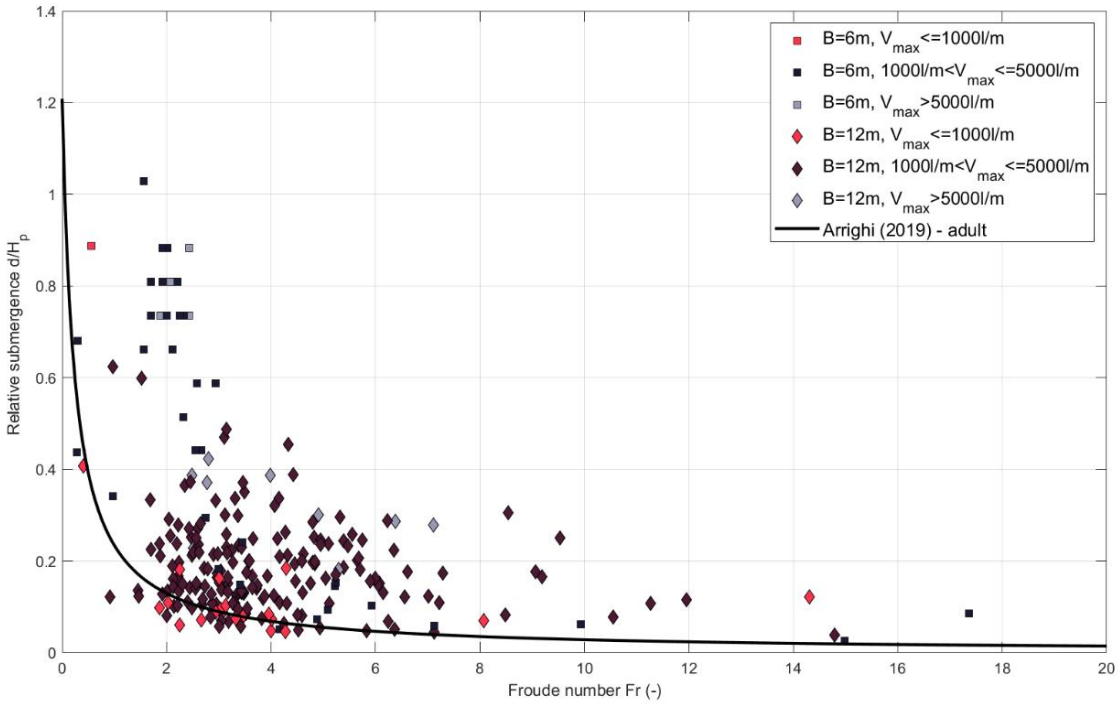

Figure 17. Froude number versus relative submergence, comparison with Arrighi (2017) curve, the discharges are divided for different promenades and maximum volumes.

7. Conclusions

In this study, 243 physical model tests of wave overtopping on smooth sea dike in very and extremely shallow water conditions have been carried out in the CIEMito wave flume at LIM/UPC. Two different foreshore slopes have been tested, 1:15 and 1:30 respectively. The dike has a crest or promenade at the end of which velocity and flow depth are measured. Overtopping volumes are collected right after the promenade. The experimental campaign aimed at modelling sea states that characterize an urbanized stretch of a town along the Catalan coast located a few kilometers north from Barcelona, where a promenade/bike path and a railway running along the coastline are exposed to significant overtopping waves every stormy season.

Overtopping flow properties were measured by means of a redundant system that consists in two ultrasonic sensors and two high-speed cameras. Velocity and depth of the maximum overtopping event characterizing each test have been measured. They prove to be dependent on the associated individual volume, crest freeboard and promenade width, however correlation is weak especially for the steeper foreshore cases. No clear correlation with mean discharge is found.

Two different methods to evaluate people safety have been used: tolerable limits for mean discharges and volumes as proposed in [6] from one side, vulnerability of pedestrian expressed as critical combination of flow velocity and depth [12]–[14]. The outcomes of the two criteria have been compared and discussed.

The results of the experimental campaign are specific for the studied area; however, some general conclusions can be drawn:

- tolerable discharge value proposed by [6] vary depending on the local wave height at the toe of the coastal structure. On the contrary, a fix value corresponding to 600 l/m is reported as threshold for individual overtopping volume. It is not clear from [6] whether this value corresponds to some specific value of overtopping flow velocity as, for example in [5]. If one criterion is fulfilled, it can happen that the other criteria appear stronger. For the case of study, average discharges were always within the proposed limits, whereas individual volumes were above the tolerable value.
- overtopping flow velocities and depths are plotted along with the corresponding maximum volumes and average discharges. What emerges is a not clear two-way relationship between maximum overtopping volumes and velocities or flow depth: A dependence does exist, as also confirmed by applying the EPR technique [27] to the present dataset. Nevertheless, the data scatter is big, therefore larger dataset is required to performed more detailed regression analysis on the data.
- experimental values of overtopping flow velocities and flow depth have been compared with stability curves for pedestrians (adults and children) placed on the sea dike and subjected to overtopping waves. Results have shown a clear influence of the dike crest width, where for mean discharges lower than 5 l/s/m and volumes lower than 1000 l/m a shorter crest does not necessarily lead to safe conditions, where the longer crest shows combination of values of overtopping flow parameters lower than the thresholds calculated using [12] or [13].
- volumes bigger than 600 l/m do not always determine unsafe conditions for pedestrian. At least the 20% of all analyzed data are in the safe region, for the specific case of study.
- EurOtop [6] tolerable limits and stability curves lead to discordant results. In fact, due to the not two-way relationship between volumes and corresponding flow parameters, it can be observed that flow parameters related to 1000 l/m maximum volumes can be located in the unsafe area, while the same parameters related to bigger volumes can even be included in the safety range for crest large enough.

Concluding, the experimental campaign suggests that further research is needed in terms of design criteria for wave overtopping, if related to people safety. Proposed tolerable discharge and volume values from the [6] are still valid but not sufficient to identify clearly a safe or unsafe scenario. Overtopping flow depth and velocity provide further insight and are advised to be employed, together with [6] criteria, for coastal safety assessment.

Author Contributions: Conceptualization, C.A. and X.G.; methodology, C.A.; validation, C.A., T.S.; formal analysis, C.A., G.V. and A.S.; investigation, C.A., T.S.; resources, X.G.; data curation, C.A.; writing—original draft preparation, C.A.; writing—review and editing, C.A, X.G., T.S., G.V., A.S.; supervision, X.G., G.V.; project administration, C.A.; funding acquisition, X.G. All authors have read and agreed to the published version of the manuscript.

Funding: This research was funded by European Union's Horizon 2020 research and innovation programme under the Marie Sklodowska-Curie grant agreement No.: 792370.

Disclaimer: The presented results reflect only the authors' view and Research Executive Agency (REA) is not responsible for any use that may be made of the information it contains.

Acknowledgments: The authors would like to acknowledge the students Mauro Campagnola and Maria Luigia Robustelli, who carried out the experimental campaign under the guidance and supervision of C.A, and the technical/research staff of LIM/UPC, in particular Joaquim Sospedra, Oscar Galego and Dr. José M. Alsina for their support and assistance for the model constructions and setup of measurement systems.

Conflicts of Interest: The authors declare no conflict of interest.

References

1. Owen.Design of seawalls allowing for wave overtopping. Hydraulics Research, Wallingford, Report No. EX 924, UK, **1980** .
2. Bruce,T.; van der Meer,J. W.; Franco,L.; and Pearson,J. M.Overtopping performance of different armour units for rubble mound breakwaters. *Coast. Eng.* **2009** , *vol. 56*, no. 2.pp. 166–179.doi: 10.1016/j.coastaleng.2008.03.015.
3. van der Meer,J. W. and Bruce,T.New Physical Insights and Design Formulae on Wave Overtopping at Sloping and Vertical Structures. *J. Waterw. Port, Coastal, Ocean Eng.* **2013** , no. i.p. 130701223023001.doi: 10.1061/(ASCE)WW.1943-5460.0000221.
4. van Gent,M. R. A.Physical model investigations on coastal structures with shallow foreshores: 2D model tests with single and double-peaked wave energy spectra, **1999** .
5. Allsop,N. W. H.; Bruce,T.; Pullen,T.; and van der Meer,J.Direct Hazards From Wave Overtopping – the Forgotten Aspect of Coastal Flood Risk Assessment? *43rd DEFRA Flood Coast. Manag. Conf.* **2008** , no. July.pp. 1–11.
6. EurOtop.*Manual on wave overtopping of sea defences and related structures. An overtopping manual largely based on European research, but for worldwide application*, **2018**. Van der Meer, J.W., Allsop, N.W.H., Bruce, T., De Rouck, J., Kortenhaus, A., Pullen, T., Schüttrumpf.
7. Schüttrumpf,H.Prediction of wave overtopping flow parameters on the crest and landward slope of seadikes. **2001** , no. April.
8. Schüttrumpf,H. and Oumeraci,H.Scale and Model Effects in Crest Level Design, in *Proc. 2nd Coastal Symposium.*, 2005, 2005, pp. 1–12.
9. Quvang,J.; Nørgaard,H.; Lykke,T.; Burcharth,H. F.; and Jan,G.Analysis of overtopping fl ow on sea dikes in oblique and short-crested waves. *Coast. Eng.* **2013** , *vol. 76*.pp. 43–54.doi: 10.1016/j.coastaleng.2013.01.012.
10. Mares-Nasarre,P.; Argente,G.; Gómez-Martín,M. E.; and Medina,J. R.Overtopping layer thickness and overtopping flow velocity on mound breakwaters. *Coast. Eng.* **2019** , *vol. 154*, no. September.doi: 10.1016/j.coastaleng.2019.103561.
11. Endoh,K. and Takahashi,S.Numerically Modeling Personnel Danger on a Promenade Breakwater Due to Overtopping Waves, in *Coastal Engineering 1994*, 1995, 1995, pp. 1016–1029, doi: 10.1061/9780784400890.075.
12. Sandoval Claudio. and Bruce Tom.Wave overtopping hazard to pedestrians: video evidence from real

accidents, in *Coasts, Marine Structures and Breakwaters 2017*, 2017, 2017, pp. 501–512, doi: 10.1680/cmsb.63174.0501.

13. Arrighi,C.; Pregnolato,M.; Dawson,R. J.; and Castelli,F.Preparedness against mobility disruption by floods. *Sci. Total Environ.* **2019** , *vol. 654*.pp. 1010–1022.doi: 10.1016/j.scitotenv.2018.11.191.
14. Arrighi,C.; Oumeraci,H.; and Castelli,F.Hydrodynamics of pedestrians' instability in floodwaters. *Hydrol. Earth Syst. Sci.* **2017** , *vol. 21*, no. 1.pp. 515–531.doi: 10.5194/hess-21-515-2017.
15. van Bergeijk,V. M.; Warmink,J. J.; van Gent,M. R. A.; and Hulscher,S. J. M. H.An analytical model of wave overtopping flow velocities on dike crests and landward slopes. *Coast. Eng.* **2019** , *vol. 149*.pp. 28–38.doi: https://doi.org/10.1016/j.coastaleng.2019.03.001.
16. Schüttrumpf,H. and Oumeraci,H.Overtopping Flow Parameters on the inner slope of Seadikes. **2002** .
17. Hughes,S. A.Hydraulic Parameters of Overtopping Wave Volumes, *Coastal Structures and Solutions to Coastal Disasters 2015*, **15 08, 2015**. pp. 710–718, **15 08, 2015**, doi: doi:10.1061/9780784480304.075.
18. Trung,L. H.Velocity and water-layer thickness of overtopping flows on sea dikes. Communications on Hydraulic and Geotechnical Engineering 2014-02 ISSN 0169-6548, **2014** . [Online]. Available: http://resolver.tudelft.nl/uuid:546471cd-4d03-48fe-a6cd-361cf81230cb.
19. Hughes,S.A. Wave momentum flux parameter: a descriptor for nearshore waves. *Coast. Eng.* **2004** , *vol. 51*, no. 11–12.pp. 1067–1084.doi: 10.1016/j.coastaleng.2004.07.025.
20. Hofland,B.; Chen,X.; Altomare,C.; and Oosterlo,P.Prediction formula for the spectral wave period Tm-1,0 on mildly sloping shallow foreshores. **2017** , *vol. 123*, no. February.pp. 21–28.doi: 10.1016/j.coastaleng.2017.02.005.
21. Altomare,C.; Suzuki,T.; Chen,X.; Verwaest,T.; and Kortenhaus,A.Wave overtopping of sea dikes with very shallow foreshores. *Coast. Eng.* **2016** , *vol. 116*.doi: 10.1016/j.coastaleng.2016.07.002.
22. Hansen,N.-E. O.; Sand,S. E.; Lundgren,H.; Sorensen,T.; and Gravesen,H.Correct Reproduction of Group-Induced Long Waves, in *Coastal Engineering 1980*, **1980**, **1980**, pp. 784–800.
23. Heller,V. Scale effects in physical hydraulic engineering models. *J. Hydraul. Res.* **2011** , *vol. 49*, no. 3.pp. 293–306.doi: 10.1080/00221686.2011.578914.
24. Formentin,S. M.; Zanuttigh,B.; and van der Meer,J. W.A Neural Network Tool for Predicting Wave Reflection, Overtopping and Transmission. *Coast. Eng. J.* **2017** , *vol. 59*, no. 1.pp. 1750006–1750031.doi: 10.1142/S0578563417500061.
25. Altomare,C.; Suzuki,T.; Chen,X.; Verwaest,T.; and Kortenhaus,A.Wave overtopping of sea dikes with very shallow foreshores. *Coast. Eng.* **2016** , *vol. 116*.pp. 236–257.doi: http://dx.doi.org/10.1016/j.coastaleng.2016.07.002.
26. Schüttrumpf,H. and Van Gent,M. R.Wave overtopping at sea dikes, in *Proceedings of Coastal Structures 2003. American Society of Civil Engineers*, 2003, 2003, pp. 431–443.
27. Giustolisi,O. and Savic,D. A.A symbolic data-driven technique based on evolutionary polynomial regression. *J. Hydroinformatics*. **2006** , *vol. 8*, no. 3.pp. 207–222.doi: 10.2166/hydro.2006.020b.
28. Altomare,C.; Gironella,X.; and Laucelli,D.Evolutionary data-modelling of an innovative low reflective vertical quay. *J. Hydroinformatics*. **2013** , *vol. 15*, no. 3.p. 763.doi: 10.2166/hydro.2012.219.
29. Altomare,C. and Gironella,X.An experimental study on scale effects in wave reflection of low-reflective quay walls with internal rubble mound for regular and random waves. *Coast. Eng.* **2014** , *vol. 90*.pp. 51–63.doi: 10.1016/j.coastaleng.2014.04.002.